Proceedings of ICRC 2001: 4019 © Copernicus Gesellschaft 2001

ICRC 2001

Atmospheric electric field effect in different neutron multiplicities according to Emilio Segre' Observatory one minute data

L. I. Dorman[1,2], I. V. Dorman[3], N. Iucci[4], Yu. Ne'eman[5], L. A. Pustil'nik[1], A. Sternlieb[1], G. Villoresi[4], and I. G. Zukerman[1]

[1]Israel Cosmic Ray Center and Emilio Segre' Observatory, affiliated to Tel Aviv University, Technion and Israel Space Agency, Israel
[2]IZMIRAN, Russian Academy of Science, Troitsk, Moscow region, Russia
[3]Institute of History of Science and Technology, Russian Academy of Science, Moscow, Russia;
[4]Dipartimento di Fisica "E. Amaldi", Universit "Roma Tre", Rome, Italy
[5]Tel Aviv University and Israel Space Agency

Abstract. On the basis of cosmic ray and atmospheric electric field one minute data obtained by NM and EFS of Emilio Segre' Observatory (hight 2025 m above s.l., cut-off rigidity for vertical direction 10.8 GV) we determine the atmospheric electric field effect in CR for total neutron intensity and for multiplicities m≥1, m≥2, m≥3, m≥4, m≥5, m≥6, m≥7, and m≥8, as well as for m=1, m=2, m=3, m=4, m=5, m=6, and m=7. For comparison and excluding primary CR variations we use also data obtained by NM of University "Roma Tre" (about sea level, cut-off rigidity 6.7 GV). According to the theoretical calculations of Dorman and Dorman (1995) the electric field effect in the NM counting rate must be caused mainly by catching of slow negative muons by lead nucleus with escaping few neutrons. As it was shown in Dorman et al. (1999), the biggest electric field effect is expected in the multiplicity m=1, much smaller in m=2 and negligible effect is expected in higher multiplicities. We will control this conclusion on the basis of our experimental data. Obtained results give a possibility to estimate total acceleration and deceleration of CR particles by the atmospheric electric field.

1. Introduction.

The atmospheric electric field effect in cosmic rays was discovered in Alexeenko et al. (1985, 1987) by 4-minute data of cosmic ray muon component intensity measured with very high accuracy (the effective area of detector for muons with threshold energy 90 *MeV* was about 200 m^2 and for muons with threshold energy 20 *MeV* was about 6.9 m^2). The atmospheric electric field effect in muon component is mostly compensated because this effect for positive and negative particles has opposite sign. The small effect we can observe only because the flux of positive particles is little bigger than negative particles (positive excess in secondary components of cosmic rays). The physical sense and general theory of this effect were discussed in Dorman (1987) and calculations of expected effect were made in Dorman & Dorman (1995), taking into account muon positive excess in dependence of particle energy and theory of muon component meteorological effects (Dorman, 1957, 1972). In Dorman & Dorman (1995, 1972) was shown also that atmospheric electric field effect must be also in the neutron monitor counting rate time variations, caused by soft negative muons captured by lead nucleus with formatting mesoatoms and then with generation of additional number of neutrons detected as neutrons from galactic cosmic rays.

2. Expected Atmospheric Electric Field Effect in Total Counting Rate of NM and in Different Multiplicities.

The atmospheric electric field effect is caused mostly by soft negative muons formatted lead mesoatoms with following ejecting of neutrons. Let us consider data on the frequency of lead mesoatoms formation in neutron monitor in dependence of multiplicity, cut-off rigidity and altitude. According to Nobles et al. (1967), the relative part of counting rate caused by formation of lead mesoatoms on the sea level is 8.94% for the multiplicity *m*=1, 6.7% for *m*=2 and 2.6% for *m*=3. For the mountain level (about 3 km) the relative part of counting rate caused by formation of lead mesoatoms is few times smaller: 1.65% for the multiplicity *m*=1, 0.68% for *m*=2 and only 0.3% for *m*=3. According to these data, the biggest atmospheric electric field effect is expected on sea level for the multiplicities *m* =1 and *m* =2. On the mountain level the atmospheric electric field effect is expected about 5 times smaller. Results of Nobles et al. (1967) were obtained for the middle cut-off rigidity ($R_C \approx 4 \div 5\,GV$) and low solar activity (near 1965). The relative part of neutron monitor counting rate caused by formation of lead mesoatoms is proportional to muon component intensity and inverse proportional to nucleonic component intensity.

· *Correspondence to*: Lev I. Dorman
(lid@physics.technion.ac.il, lid1@ccsg.tau.ac.il)

The muon component intensity decreases from $R_c \le 2\,GV$ to $R_c \approx 15\,GV$ only on about 10% but intensity of neutron component decreases on about 50%. It means that the relative part of neutron monitor counting rate caused by formation of lead mesoatoms is expected to be increase on about 40% from $R_c \le 2\,GV$ to $R_c \approx 15\,GV$, that on sea level this part will be increase from 8.9% to 12.5% for the multiplicity *m*=1, from 6.7% to 9.4% for *m* = 2 and from 2.6% to 3.6% for *m* = 3. From the minimum to the maximum of solar activity at $R_c \le 2\,GV$ intensity of muon component decreases on about 6% and neutron component on about 20%; it means that the relative part of neutron monitor counting rate caused by formation of lead mesoatoms expected to be increase on about 14% from minimum to maximum of solar activity. Near equator this increasing will be smaller.

According to Dorman & Dorman (1999), expected atmospheric electric field effect can be described by

$$\left(\frac{\Delta I_k^i(t)}{I_{ko}^i}\right)_E = \int_0^{h_o} \Delta E(h,t)\,\boldsymbol{\alpha}_E^i(h,R_c,h_o)\,dh, \qquad (1)$$

where $\Delta E(h,t)$ is the vertical component of atmospheric electric field variation from the top of atmosphere (*h*=0) to the bottom on the level of observation h_o (mostly it is between the level h_o and level of clouds about 3-5 *km*), and

$$\Delta E(h,t) = E(h,t) - E_o(h). \qquad (2)$$

According to Dorman & Dorman (1999), for observations on sea level in the period of low solar activity on high and middle latitudes

$$\boldsymbol{\alpha}_E^{1,2,3} \approx (11.6;\ 8.7;\ 3.4)\times 10^{-5} (kV/m)^{-1} \left(g/cm^2\right)^{-1}\% \qquad (3)$$

correspondingly for multiplicities *m*=1, 2 and 3.

With increasing of solar activity the total atmospheric electric field coefficients will be little increase, that at the maximum of solar activity instead of Eq. (3) we obtain

$$\boldsymbol{\alpha}_E^{1,2,3} \approx (12.5;\ 9.4;\ 3.6)\times 10^{-5} (kV/m)^{-1} \left(g/cm^2\right)^{-1}\%. \qquad (4)$$

With increasing of cut-off rigidity the total atmospheric electric field coefficients will be bigger; for example, for the period of low solar activity near equator the total atmospheric electric field coefficients will be:

$$\boldsymbol{\alpha}_E^{1,2,3} \approx (16.2;\ 12.2;\ 4.7)\times 10^{-5} (kV/m)^{-1} \left(g/cm^2\right)^{-1}\%. \qquad (5)$$

With increasing of altitude of observations, the total atmospheric electric field coefficients decrease sufficiently. For example, for observations on mountains (about 3 *km*) in the period of low solar activity on high and middle latitudes

$$\boldsymbol{\alpha}_E^{1,2,3} \approx (2.1;\ 0.9;\ 0.4)\times 10^{-5} (kV/m)^{-1} \left(g/cm^2\right)^{-1}\%. \qquad (6)$$

3. Periods of Thunderstorms on Mt. Hermon

In Table 1 are shown periods of thunderstorms on Mt. Hermon, their times of start and finish, total duration and maximum of atmospheric electric field observed with the EFS-detector of Emilio Segre' Observatory in each period.

Table 1. List of thunderstorms periods on Mt. Hermon

Case	Start, UT	Finish, UT	Duration, min	Vmax, kV/m
1	05 02 00 15:10	06 02 00 03:25	735	34
2	12 02 00 17:36	13 02 00 08:44	908	110
3	13 02 00 17:32	14 02 00 00:20	408	54
4	15 02 00 18 39	16 02 00 12:42	1083	80
5	19 02 00 11:55	19 02 00 19 16	441	36
6	22 02 00 14:43	23 02 00 03:56	793	48
7	27 02 00 11:31	27 02 00 12 31	60	14
8	01 03 00 01:05	01 03 00 18:22	1037	112
9	04 03 00 09:04	04 03 00 14:45	341	64
10	06 03 00 20:25	07 03 00 02:16	351	16
11	08 04 00 17:35	08 04 00 20:10	155	26
12	08 04 00 22:59	09 04 00 06:07	428	70
13	09 04 00 10:51	09 04 00 18:38	467	56
14	19 04 00 01:49	19 04 00 02:46	57	26
15	20 04 00 01:42	20 04 00 04:48	186	56
16	03 05 00 21:19	04 05 00 00:11	172	10
17	08 05 00 06:08	08 05 00 07:38	90	8
18	22 10 00 21:51	23 10 00 04:18	387	12
19	23 10 00 10:18	23 10 00 12:23	125	22
20	23 10 00 14:58	24 10 00 15:23	1465	70
21	25 10 00 01:34	25 10 00 07:07	333	10
22	25 10 00 11:59	25 10 00 14:55	176	14
23	29 11 00 05:31	29 11 00 06:20	49	10
24	29 11 00 18:23	30 11 00 05:11	648	20
25	30 11 00 14:09	01 12 00 03:10	781	50
26	12 12 00 08:27	13 12 00 07:15	1368	80
27	19 12 00 01:20	20 12 00 22:09	2689	88
28	24 12 00 09:00	24 12 00 13:39	279	30
29	02 01 01 15:03	03 01 01 04:10	787	26
30	17 01 01 10:41	17 01 01 13:12	151	76
31	18 01 01 14:49	19 01 01 01:14	625	70
32	19 01 01 06:45	19 01 01 15:26	521	50
33	19 01 01 23:56	20 01 01 01:11	75	14
34	23 01 01 18:58	25 01 01 05:58	2100	62
35	03 02 01 06:47	04 02 01 18:21	2134	88
36	13 02 01 20:52	15 02 01 01:12	1700	60
37	15 02 01 12:45	15 02 01 15:44	179	24
38	20 02 01 00:09	20 02 01 23:21	1392	48
39	23 02 01 12:24	23 02 01 13:36	72	40
40	14 03 01 01:19	14 03 01 01:52	33	12
41	23 03 01 22:54	24 03 01 01:58	184	72
42	02 04 01 13:43	02 04 01 16:07	144	40
43	07 04 01 13:45	07 04 01 15:02	77	52
44	01 05 01 20:16	02 05 01 01:32	316	16
45	02 05 01 08:57	02 05 01 09:49	52	40
46	09 05 01 04:44	09 05 01 05:11	27	28
47	09 05 01 07:58	09 05 01 10:10	132	20
48	13 05 01 03:30	13 05 01 03:58	28	20
49	13 05 01 04:45	13 05 01 07:33	168	40

From Table 1 can be seen that several times was observed very high atmospheric electric field characterized by $E_{\max} = 80 \div 110\,kV/m$. This field is very dangerous for neutron monitor, electronics and computers in our Observatory. To save our Observatory from this dangerous electric field we used ground connected Faraday net-protector. In Fig. 1 are shown values $E_{\max}$ in dependence from thunderstorms period duration *T*.

From Fig. 1 can be seen that there are clear tendency of increasing of $E_{\max}$ with increasing of thunderstorms period duration *T* (in minutes):

Figure 1. E_{max} vs thunderstorms periods duration.

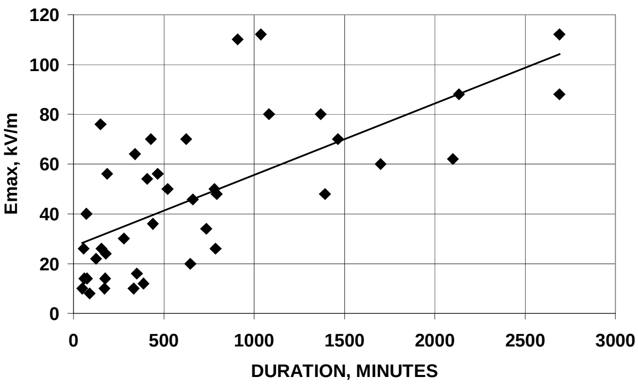

$$E_{max} = 0.029T + 27\, kV/m \qquad (7)$$

with correlation coefficient 0.68.

4. Examples of Atmospheric Electric Field Variations on Mt. Hermon

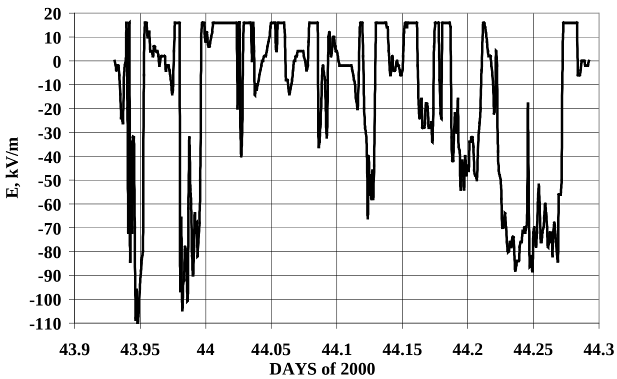

Figure 2. One-minute data of atmospheric electric field on Mt. Hermon in one of periods of thunderstorms in February 2000.

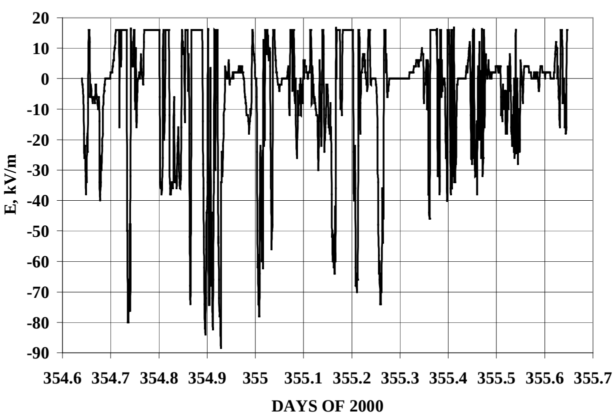

Figure 3. The same as in Fig. 2, but in December 2000.

The sensor of atmospheric electric field EFS-1000 starts to work in our Observatory on Mt. Hermon in February 2000. It made measurements each minute for negative field up to –160 kV/m and for positive field up to +16 kV/m. In Fig. 2 and 3 are shown examples of these measurements.

5. Regression Relations between Atmospheric Electric Field and Counting Rates in ESO NM for Total and Different Multiplicities.

To our pity, for regression analysis we cannot use directly theoretical Eq. (1) because information on the space-time distribution of atmospheric electric field $\Delta E(h,t)$ now is not available. In Emilio Segre' Observatory on Mt. Hermon we

have one-minute data of continuously measurements only $\Delta E(h_o,t)$ in the place occupied by our Observatory. We suppose that approximately $\Delta E(h_o,t)$ is in good correlation with distribution function $\Delta E(h,t)$. In this case instead of Eq. (1) we obtain,

$$\left(\Delta I_k^i(t)\big/ I_{ko}^i\right)_E = \alpha_E^i \times \Delta E(h_o,t) + Const, \qquad (8)$$

where

$$\alpha_E^i \approx \int_{h_o}^{h_{max}} \alpha_E^i(h)dh \;. \qquad (9)$$

Here h_{max} means the air pressure on altitude of charged clouds caused thunderstorms. According to Eq. (8) we can made regression analysis. Because the expected atmospheric electric field effect for measurements by NM on mountain heights is very small (see above, Section 2), it is necessary to decrease fluctuations in cosmic ray intensity caused by other causes then atmospheric electric field effects. That we corrected data of total and different multiplicities on barometric effect (see in Dorman et al., 2001a), on snow effect (Dorman et al., 2001b), and on primary variations (by using Rome NM data for comparison). As example, here we present results of regression analysis for 7 periods of February 2000 (total duration of thunderstorms periods more than 5000 minutes). Our EFS-1000 for all E > +16 kV/m gives the same value as at E = +16 kV/m. Therefore we excluded from regression analyses all points with E = +16 kV/m. Especially relative great scattering of points we have at smaller values of E when the atmospheric electric field effects in NM total and multiplicities intensities are negligible. To reduce influence of these points, we also excluded them. In Fig. 4-7 are shown CR intensity variations vs atmospheric electric field E for total intensity and multiplicities m=1, 2 and 3 in the case when are excluded points with $|E| \le 2\,kV/m$. Fig. 4-7 show a great scattering of points even after eliminated of all variations caused by non atmospheric electric field effects. But let us remember that in Fig. 4-7 are shown one-minute data characterized with statistical errors 0.98%, 1.45%, 2.76% and 4.74% for total intensity and multiplicities m=1, 2, 3.

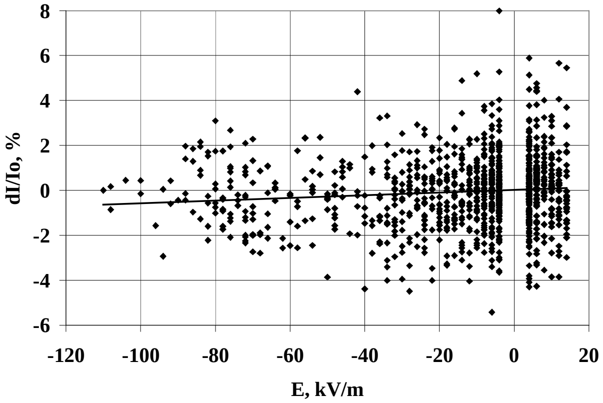

Figure 4. NM counting rate dependence from atmospheric electric field E for total neutron intensity. The linear regression is shown by straight line.

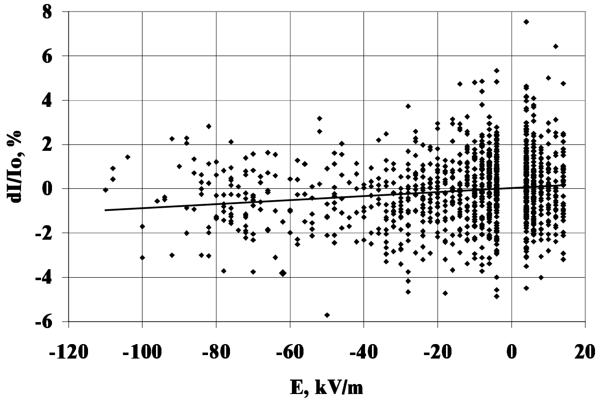

Figure 5. The same as in Fig. 4, but for m=1.

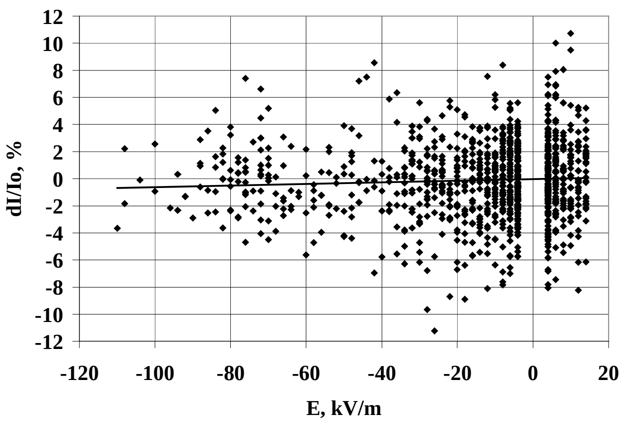

Figure 6. The same as in Fig. 4, but for m=2.

In Table 2 are shown results of regression analysis

$$dI/I_o = A \times E + Const \qquad (10)$$

for case C when all data are used, cases C-0, C-2, C-4 and C-6 for excluded data with E=0, $|E| \le 2, \le 4, \le 6\, kV/m$, correspondingly.

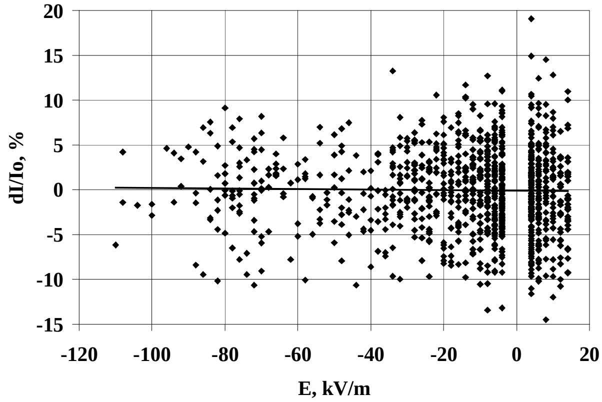

Figure 7. The same as in Fig. 4, but for m=3.

Table 2. Regression coefficients A in %/(kV/m) and relative statistical errors $R=\sigma(A)/A$ for 7 thunderstorms periods in February 2000.

Chan-nel	case	C	C-0	C-2	C-4	C-6
	No min	5137	2026	1141	836	678
total	*A*	4.2E-03	5.8E-03	6.0E-03	6.4E-03	5.9E-03
	R	3.8E-02	3.4E-02	3.0E-02	2.2E-02	1.4E-02
m=1	*A*	7.2E-03	8.6E-03	9.1E-03	8.8E-03	9.1E-03
	R	3.8E-02	3.4E-02	2.9E-02	2.2E-02	1.4E-02
m=2	*A*	4.2E-03	7.3E-03	5.9E-03	7.0E-03	6.5E-03
	R	3.8E-02	3.5E-02	3.0E-02	2.2E-02	1.4E-02
m=3	*A*	3.0E-05	-3.2E-03	-3.1E-03	-2.3E-05	-1.2E-03
	R	3.8E-02	3.5E-02	3.0E-02	2.2E-02	1.4E-02

6. Discussion and Conclusions.

Let us compare obtained in Section 5 results with theoretically expected (Section 3). If we suppose that atmospheric electric field is prolonged on about 3-4 km (about 300 g/cm^2 , that from Eq. (6) for observations on 3 km with taking into account Eq. (9), we obtain

$$A_{exp} \approx 6.3\times10^{-3}, 2.7\times10^{-3}, 1.2\times10^{-3}\ \%/(kV/m) \qquad (11)$$

for m=1, 2, 3. For Mt. Hermon (about 2 km) expected A will be little bigger, what in first approximation is in good agreement with obtained results (see Table 2). It is important that the biggest A we obtained for m=1 and much smaller for m=3, in agreement with theory (Dorman and Dorman. 1999)

References

Dorman, L.I. and Dorman I.V., Canadian J. Phys. **73**, 440, 1995.
Dorman, L.I. and Dorman I.V.., Proc. 26th ICRC**, 7**, 309, 1999.
Dorman, L.I. et al., Proc. 26th ICRC**, 7**, 425, 1999.